

¹ Chainsweep-based efficiency of bottom trawl surveys and biomass
² estimates for flatfish, red hake, and goosefish stocks in Northwest
³ Atlantic waters of the United States

⁴ Timothy J. Miller¹, David E. Richardson², Andrew Jones², Phil Politis¹

⁵ ¹timothy.j.miller@noaa.gov, Northeast Fisheries Science Center, National Marine Fisheries Service, 166 Water
⁶ Street, Woods Hole, MA 02543, USA

⁷ ²Northeast Fisheries Science Center, National Marine Fisheries Service, Narragansett, RI USA

9 Abstract

10 Using a general hierarchical model we estimated relative efficiency of chain sweep to the rockhopper sweep
11 used by the NEFSC bottom trawl survey for from studies carried out between 2015 and 2017 aboard the
12 F/V Karen Elizabeth twin-trawl vessel. Aside from the sweeps, the rest of the trawl gear is the same. We
13 compared a set of models with different assumptions about variation of relative efficiency between paired
14 gear tows, size and diel effects on the relative efficiency, and extra-binomial variation of observations within
15 paired gear tows.

16 Using a general hierarchical model we estimated relative efficiency of chain sweep to the rockhopper sweep
17 used by the NEFSC bottom trawl survey for winter and windowpane flounder stocks and red hake stocks from
18 studies carried out between 2015 and 2017 aboard the F/V Karen Elizabeth twin-trawl vessel. Aside from
19 the sweeps, the rest of the trawl gear is the same. We compared a set of models with different assumptions
20 about variation of relative efficiency between paired gear tows, size and diel effects on the relative efficiency,
21 and extra-binomial variation of observations within paired gear tows. Diel effects provided improved model
22 performance for all three species. We used the best performing model to make annual chain sweep-based swept
23 area biomass and abundance-at-length estimates. We estimated uncertainty in all results using bootstrap
24 procedures for each data component.

25 Keywords

26 hierarchical models, spline regression, gear efficiency, abundance estimation

²⁷ 1 Introduction

²⁸ Paired-gear studies have long been used to estimate the efficiency of one fishing gear relative to another (e.g.,
²⁹ Gulland, 1964; Bourne, 1965). These types of studies are critical for informing abundance time series from
³⁰ fishery independent surveys when there are changes in the vessel and(or) gears over time due to gear failures
³¹ or improved technology.

³² Within the northeast US there has been a heightened focus on trawl survey operations and gear efficiency.
³³ This focus has in part resulted from low quotas for a number of grounfish limiting fishing opportunities.
³⁴ To help provide clarity on the trawl operations and build trust in survey indies the New England Fisheries
³⁵ Management Council developed a Northeast Trawl Advisory Panel. This panel is composed of members from
³⁶ industry, regional academics, as well as state and federal scientists. Together the group designed a set of
³⁷ experiments to explore the differences in efficiency between survey and trawl gear (hereafter referred to as
³⁸ ‘chain sweep’ experiments).

³⁹ The goal of these chain sweep experiments was to provide estimates of what absolute abundance might be, so
⁴⁰ that this could be used for assessment processes. For example, developing an estimate of absolute abundance
⁴¹ allows for some swept-area biomass calculations at the region scale. These estimates can then be compares
⁴² to other index-based empirical assessment methods. This is especially valuable for species where limited
⁴³ commercial harvest occurs, but assessments suggest the species is in poor status (e..g, red hake).

⁴⁴ In conducting paired-gear studies it is ideal to have the two gears deployed as close together spatially and
⁴⁵ temporally as possible to reduce variation between the gears in densities of the species being captured.
⁴⁶ One fishing method that approaches this ideal is the twin-trawl rigging where two trawls can be fished
⁴⁷ simultaneously (ICES, 1996). The basic methods we used here are based on those used by Miller (2013)
⁴⁸ to estimate size effects on relative catch efficiency of the Henry B. Bigelow to the Albatross IV. Similar
⁴⁹ approaches were used to make similar estimates for groundfish, TRAC stocks and summer flounder (Miller
⁵⁰ et al., 2017a,b). The methods here are the same as those used for red hake for the red hake research track
⁵¹ assessments (Miller et al., 2020).

⁵² Importance of biomass or (catchability) efficiency estimates for both index-based methods as well as age-
⁵³ structured models with low contrast.

54 **2 Methods**

55 **2.1 Data collection**

56 Data were collected during three field experiments carried out in 2015, 2016, and 2017, respectively, aboard
57 the F/V Karen Elizabeth, a 78ft stern trawler capable of towing two trawls simultaneously side by side.
58 However, red hake were only observed during the 2017 field experiments. One side of the twin-trawl rig
59 towed a NEFSC standard 400 x 12 cm survey bottom trawl rigged with the NEFSC standard rockhopper
60 sweep (Politis et al., 2014) (Figure 1). The other side of the twin-trawl rig towed a version the NEFSC 400 x
61 12cm survey bottom trawl modified to maximize the capture of flatfish. The trawl was modified by reducing
62 the headline flotation from 66 to 32, 20cm, spherical floats, reducing the port and starboard top wing-end
63 extensions by 50cm each and utilizing a chain sweep. The chain sweep was constructed of 1.6cm (5/8in) trawl
64 chain covered by 12.7cm diameter x 1cm thick rubber discs on every other chain link (Figure 2). Two rows of
65 1.3cm (1/2in) tickler chains were attached to the 1.6cm trawl chain by 1.3cm shackles (Figure 2). To ensure
66 equivalent net geometry of each gear, 32m restrictor ropes, made of 1.4cm (9/16in) buoyant, Polytron rope,
67 were attached between each of the trawl doors and the center clump. 3.4m² Thyboron Type 4 trawl doors
68 were used to provide enough spreading force to ensure the restrictor ropes remained taut throughout each
69 tow. Each trawl used the NEFSC standard 36.6m bridles. All tows followed the NEFSC standard survey
70 towing protocols of 20 minutes at 3.0 knots. In 2015, 108 (45 day, 63 night) paired tows were conducted in
71 eastern Georges Bank and off of southern New England (Figure 3). In 2016, 117 (74 day, 43 night) paired
72 tows were conducted in western Gulf of Maine and northern edge of Georges Bank (Figure 4). In 2017, 103
73 (61 day, 42 night) paired tows were conducted in waters off of southern New England (Figure 5). Paired tows
74 were denoted as “day” and “night” by whether the sun was above or below the horizon at the time of the tow.

75 Winter flounder were caught in 171 paired tows (97 day, 74 night). Overall 6,449 winter flounder were
76 measured for length. The subsampling fractions implied an estimated 6,586 winter flounder were captured
77 across all paired tows. 3805 and 2644 length measurements were made for the chainsweep and rockhopper
78 gears, respectively. During the day, 2385 and 1220 winter flounder were measured in catches by the respective
79 gears whereas during the night 1420 and 1424 were measured in catches by the respective gears.

80 Windowpane flounder were caught in 195 paired tows (100 day, 95 night). Overall 13,014 windowpane were
81 measured for length. The subsampling fractions implied an estimated 15,310 windowpane were captured
82 across all paired tows. 9854 and 3160 length measurements were made for the chainsweep and rockhopper
83 gears, respectively. During the day, 5443 and 778 windowpane were measured in catches by the respective

84 gears whereas during the night 4411 and 2382 were measured in catches by the respective gears.

85 Red hake were caught in 73 paired tows (40 day, 33 night). Overall 12,585 red hake were measured for length.

86 The subsampling fractions implied an estimated 47,275 red hake were captured across all paired tows. 8587

87 and 3998 length measurements were made for the chainsweep and rockhopper gears, respectively. During the

88 day, 4908 and 1706 red hake were measured in catches by the respective gears whereas during the night 3679

89 and 2292 were measured in catches by the respective gears.

90 2.2 Paired-tow analysis

91 We use the hierarchical modeling approach from Miller (2013) to estimate the relative efficiency of chain

92 sweep to the rockhopper sweep used by the NEFSC bottom trawl survey for six species from three studies

93 carried out aboard a twin trawl vessel. Aside from the sweeps the rest of the trawl gear is the same. As in

94 Miller (2013), we compared a set of models with different assumptions about variation of relative efficiency

95 between paired gear tows, size effects on the relative efficiency, and extra-binomial variation of observations

96 within paired gear tows. We began with the same 13 models considered by Miller (2013). Models BI₁ to BI₄

97 and BB₁ to BB₈ in Table ?? provides a descriptions of the models fitted for all species and pseudo-formulas

98 comparable to those used for fitting models in R and the mgcv package (R Core Team, 2019; Wood, 2006).

99 We then also included diel effects on relative catch efficiency and interactions with size effects with the

100 best performing model of the original 13 models for each species. For red hake, these are the same analyses

101 provided in Miller et al. (2020) and the new analyses for winter and windowpane flounder are analogous. The

102 analyses here and in Miller et al. (2020) are similar to those by Miller et al. (2017a), Miller et al. (2017b),

103 and Miller et al. (2018), but a more generalized model has been implemented that allows multiple smooth

104 effects on relative catch efficiency so that models do not have to be fit separately to observations occurring

105 during the day and night. Therefore, diel effects on relative catch efficiency and interactions with size effects

106 can be considered while allowing other parameters to be the same for all observations.

107 Also, we used the Template Model Builder package (Kristensen et al., 2016) in R to program the models and

108 the “nlminb” optimizer to fit the models (?).

109 If the best model included regression splines of length and smooth parameters estimated linear functions of

110 length (on the transformed scale), then simpler linear models were assumed for further models that included

111 diel effects on relative efficiency. One less parameter (smoothing parameter) for these models.

112 To estimated uncertainty in relative catch efficiency two ways. First we used the inverted hessian of the

113 marginal log-likelihood and the delta-method to estimate uncertainty in the predicted relative catch efficiency

at size. Second, we refit models to bootstrap resamples of the paired station data. Specifically, we resampled the paired tows so that the total number paired tows was the same for a given species, but the total number of length measurements varied depending on which of the paired tows entered the sample for a particular bootstrap. We made 1000 bootstrap samples and estimated relative catch efficiency at size from each bootstrap data set if the fitted model converged and the hessian of the maximized log-likelihood was invertible.
 Red hake: had to assume station-specific random effects that corresponded to the population-level fixed effects were uncorrelated because of convergence issues.

2.3 Length-weight analysis

We fit length-weight relationships to the length and weight observations for each survey each year. We assumed weight observation j from survey i , was log-normal distributed,

$$\log W_{ij} \sim N \left(\log \alpha_i + \beta_i \log L_{ij} - \frac{\sigma_i^2}{2}, \sigma_i^2 \right) \quad (1)$$

We used a bias correction to ensure the expected weight $E(W_{ij}) = \alpha_i L_{ij}^{\beta_i}$. We estimated parameters by maximizing the model likelihood programmed in TMB (Kristensen et al., 2016) and R (R Core Team, 2019). Like the relative catch efficiency, bootstrap predictions of weight at length were made by sampling with replacement the length-weight observations within each annual survey and refitting the length-weight relationship to each of the bootstrap data sets.

2.4 Biomass estimation

We estimated biomass for each annual survey in terms of chainsweep efficiency by scaling the survey tow observations by the relative efficiency of the chainsweep and rockhopper sweep gears. First the tow-specific catches at length are rescaled,

$$\tilde{N}_{hi}(L) = N_{hi}(L) \hat{\rho}_i(L) \quad (2)$$

where $N_{hi}(L)$ is the number at length L in tow i from stratum h and $\hat{\rho}_i(L)$ is the relative efficiency of the chain sweep to rockhopper sweep at length L estimated from the twin trawl observations, that may depend on the diel characteristic of tow i if that factor is in the best model fitted to the twin-trawl observations.
 Note that we have omitted any subscripts denoting the year or survey.

¹³⁷ The stratified abundance estimate is then calculated using the design-based estimator,

$$\widehat{N}(L) = \sum_{h=1}^H \frac{A_h}{An_h} \sum_{i=1}^{n_h} \widetilde{N}_{hi}(L) \quad (3)$$

¹³⁸ where A_h is the area of stratum h , $A = \sum_{h=1}^H A_h$, and n_h is the number of tows that were made in stratum
¹³⁹ h . The corresponding biomass estimate is then

$$\widehat{B} = \sum_{l=1}^{n_L} \widehat{N}(L = l) \widehat{w}(L = l) \quad (4)$$

¹⁴⁰ where $\widehat{w}(L = l)$ is the estimated weight at length from fitting length-weight observations described above.
¹⁴¹ Length is typically measured to the nearest cm so n_L indicates the number of 1 cm length categories that
¹⁴² were observed during the survey.

¹⁴³ To estimate uncertainty in biomass, we used bootstrap results for the relative catch efficiency and weight at
¹⁴⁴ length estimates along with bootstrap samples of the survey data. Bootstrap data sets for each of the annual
¹⁴⁵ surveys respected the stratified random designs by resampling with replacement within each stratum (Smith,
¹⁴⁶ 1997). For each of the 1000 combined bootstraps, survey observations for bootstrap b were scaled with the
¹⁴⁷ corresponding bootstrap estimates of relative cookie sweep to rockhopper sweep efficiency and predicted
¹⁴⁸ weight at length, using Eqs. 3 and 4.

¹⁴⁹ 3 Results

¹⁵⁰ All 1000 bootstrap fits of the paired tow data provided estimates of relative catch efficiency at size for summer,
¹⁵¹ windowpane, and yellowtail flounder, and red hake, goosefish, and thorny skate. All but 2 of the bootstraps
¹⁵² for winter flounder and 3 for barndoor skate provided estimates of relative catch efficiency. For witch flounder,
¹⁵³ 817 bootstraps provided estimates and only 386 provided estimates for American plaice.

¹⁵⁴ **3.1 Summer flounder**

¹⁵⁵ **3.2 American plaice**

¹⁵⁶ **3.3 Yellowtail flounder**

¹⁵⁷ **3.4 Witch flounder**

¹⁵⁸ **3.5 Goosefish**

¹⁵⁹ **3.6 Winter flounder**

¹⁶⁰ As measured by AIC, the best performing model for winter flounder before considering day/night effects was
¹⁶¹ the conditional binomial model BI₄ (Table ??). Allowing smooth size-effects on relative catch efficiency and
¹⁶² variation in these effects among paired-tows provided primary improvements in model performance. Including
¹⁶³ diel effects on relative efficiency for the twin-trawl observations improved performance of the binomial model
¹⁶⁴ (BI₅), however the model allowing the size effects on relative efficiency to differ between day and night (BI₆)
¹⁶⁵ would not converge. The relative efficiency of the chain sweep gear to the rockhopper sweep gear is greatest at
¹⁶⁶ the smallest sizes of winter flounder, but is fairly constant over over sizes greater than 25 cm. The minimum
¹⁶⁷ relative efficency is between 1.5 and 2 during the day, but efficiencies of the two sweeps are approximately
¹⁶⁸ equal efficiency at night (Figure ??).

¹⁶⁹ Stock-specific biomass estimates from 2009 to 2019 for the NEFSC spring and fall survey were variable.
¹⁷⁰ Georges Bank winter flounder biomass estimates range between 1800 and 9400 mt in the spring and 3000 and
¹⁷¹ 24,000 mt in the fall and are lower in recent years than those in the early years (Figure ?? and Table ??).
¹⁷² However, we note that the estimates of biomass made here were determined in the 2019 assessment to be
¹⁷³ problematic because of the larger sizes that predominate in the Georges Bank stock area than other stock
¹⁷⁴ areas and the low number of observations in the chainsweep study of these larger individuals (NEFSC, 2020).
¹⁷⁵ Gulf of Maine winter flounder biomass estimates are constrained to the segment of the population at least 30
¹⁷⁶ cm in length. The spring biomass estimates have been fairly stable ranging between 900 and 2700 mt whereas
¹⁷⁷ the fall estimates were greater at the beginning of the time series than recent years and range between 1900
¹⁷⁸ and 4300 mt (Figure ?? and Table ??). Southern New England winter flounder biomass estimates are also
¹⁷⁹ lower in recent years than the beginning of the time series for both seasons and spring and fall estimates
¹⁸⁰ range from 1300 to 8500 mt and 2100 to 47,500 mt, respectively (Figure ?? and Table ??).

181 The efficiency of the rockhopper gear relative to the chainsweep in terms of biomass changes from year to
182 year due primarily to corresponding changes in the estimated numbers at length (Table ??). Annual biomass
183 relative efficiency for Georges Bank winter flounder varied between 0.55 and 0.79 in the spring and 0.61 and
184 0.92 in the fall. Relative efficiencies for the Gulf of Maine stock range between 0.54 and 0.70 for the spring
185 and 0.63 and 0.88 in the fall. Relative efficiencies for the Southern New England stock range between 0.64
186 and 0.91 for the spring and 0.60 and 1.0 for the fall.

187 Because the length-weight relationship which is used with the numbers at length to estimate biomass is
188 estimated by survey and year there is a possibility that poor sampling in a given year could adversely affect the
189 biomass estimates. We therefore calculated the ratios of the annual uncalibrated biomass estimates using just
190 the aggregate catch data to the biomass estimates made using the numbers at length and estimated weight at
191 length (i.e., Eqs. 3 and 4 without the relative efficiency at size). These ratios should be approximately 1.
192 The ratios for all years and seasons for all three stocks of winter flounder varied from 0.94 to 1.04 (Table ??).

193 3.7 Windowpane flounder

194 As measured by AIC, the best performing model for windowpane flounder before considering day/night effects
195 was the conditional binomial model BI₄ (Table ??). Allowing smooth size-effects on relative catch efficiency
196 and variation in these effects among paired-tows provided primary improvements in model performance.
197 Including diel effects on relative efficiency at size for the twin-trawl observations improved performance of the
198 binomial model (BI₆). The relative efficiency of the chain sweep gear to the rockhopper sweep gear decreases
199 with size of windowpane flounder. The minimum relative efficiency is between 4.5 and 21 during the day, and
200 between 1.8 and 2.9 at night (Figure ??).

201 Stock-specific biomass estimates from 2009 to 2019 for the NEFSC spring and fall survey were variable.
202 Georges Bank-Gulf of Maine windowpane flounder biomass estimates range between 3000 and 20,300 mt in
203 the spring and 4700 and 18,300 mt in the fall and are lower in recent years than those in the early years
204 (Figure ?? and Table ??). Southern New England-Mid-Atlantic Bight windowpane flounder biomass estimates
205 in the spring ranged between 7300 and 15,600 mt whereas the fall estimates ranged between 7300 and 14,700
206 mt (Figure ?? and Table ??).

207 The efficiency of the rockhopper gear relative to the chainsweep in terms of biomass changes from year to
208 year due primarily to corresponding changes in the estimated numbers at length (Table ??). Annual biomass
209 relative efficiency for Georges Bank-Gulf of Maine windowpane flounder varied between 0.21 and 0.36 in the
210 spring and 0.19 and 0.42 in the fall. Relative efficiencies for the Southern New England-Mid-Atlantic Bight

211 stock ranged between 0.22 and 0.36 for the spring and 0.26 and 0.35 in the fall.

212 Because the length-weight relationship which is used with the numbers at length to estimate biomass is
213 estimated by survey and year there is a possibility that poor sampling in a given year could adversely affect the
214 biomass estimates. We therefore calculated the ratios of the annual uncalibrated biomass estimates using just
215 the aggregate catch data to the biomass estimates made using the numbers at length and estimated weight at
216 length (i.e., Eqs. 3 and 4 without the relative efficiency at size). These ratios should be approximately 1. The
217 ratios for all years and seasons for both stocks of windowpane flounder varied from 0.97 to 1.04 (Table ??).

218 3.8 Red hake

219 For red hake, the best performing model before considering day/night effects was the conditional beta-binomial
220 model BB₆ (Table ??). The best beta-binomial model had an AIC more than 13 units lower than the best
221 binomial model. Allowing variation in smooth size-effects on relative catch efficiency among paired-tows and
222 extra-binomial variation withing paired-tows (overdispersion via the beta-binomial assumption) provided
223 primary improvements in model performance. Including diel effects on relative efficiency for the twin-trawl
224 observations improved performance of the beta-binomial model. Initially separate smooth size effects for
225 day and night tows were considered for the beta-binomial model (BB₈), but the correlation of non-smoother
226 related random effects across stations was not estimable. Those random effects were therefore assumed
227 uncorrelated (BB₉). Allowing different smooth size effects of relative efficiency for day and night observations
228 was considerd (BB₁₀), but it did not improve model performance. The relative efficiency of the chain sweep
229 gear to the rockhopper sweep gear generally declines with increased size whether the tow occurred during day
230 or night, but the increase in efficiency of the chainsweep was generally greater for tows occuring during the
231 day (Figure ??).

232 Stock-specific trends in annual biomass estimates from 2009 to 2019 for the NEFSC spring and fall survey
233 were generally the same. For northern red hake both the spring and fall biomass estimates increased in 2014
234 and have remained higher than previous years (Figure ?? and Table ??). The scale of the biomass estimates
235 is also similar for the spring and fall surveys. For southern red hake, the spring biomass generally declined
236 until 2017 and then has increased for the last two years whereas the fall biomass has remained relatively
237 stable (Figure ?? and Table ??).

238 The efficiency of the rockhopper gear relative to the chainsweep in terms of biomass changes from year to
239 year due primarily to corresponding changes in the estimated numbers at length (Table ??). Annual biomass
240 relative efficiency for northern red hake varied between 0.19 and 0.25 in the spring and 0.21 and 0.33 in the

²⁴¹ fall. Values range between 0.15 and 0.26 for the spring and 0.19 and 0.39 in the fall for southern red hake.
²⁴² Because the length-weight relationship which is used with the numbers at length to estimate biomass is
²⁴³ estimated by survey and year there is a possibility that poor sampling in a given year could adversely affect the
²⁴⁴ biomass estimates. We therefore calculated the ratios of the annual uncalibrated biomass estimates using just
²⁴⁵ the aggregate catch data to the biomass estimates made using the numbers at length and estimated weight at
²⁴⁶ length (i.e., Eqs. 3 and 4 without the relative efficiency at size). These ratios should be approximately 1. The
²⁴⁷ ratios for all years and seasons for both northern and southern red hake varied from 0.96 to 1.04 (Table ??).

²⁴⁸ 4 Discussion

²⁴⁹ Compare greater or lesser smoothness within stations with Pedersen et al. 2019. We assume the same
²⁵⁰ number of knots and order (derivatives for penalties) in the cubic regression splines for the population and
²⁵¹ station-level smoothers. Pedersen et al. also implicitly assume the random effects that correspond to the
²⁵² null space (intercept and fixe effects of the smoothers) are uncorrelated, but correlation in these models is
²⁵³ estimated except for red hake where we found it to be inestimable.

²⁵⁴ Acknowledgements

255 **References**

- 256 Bourne, N. 1965. A comparison of catches by 3- and 4-inch rings on offshore scallop drags. Journal of the
257 Fisheries Research Board of Canada **22**(2): 313–333.
- 258 Gulland, J. A. 1964. Variations in selection factors, and mesh differentials. Journal Du Conseil International
259 Pour L'exploration De La Mer **29**(2): 158–165.
- 260 ICES. 1996. Manual of methods of measuring the selectivity of towed fishing gears. (Eds.) Wileman, D. A.,
261 Ferro, R. S. T., Fonteyne, R., and Millar, R. B. ICES Cooperative Research Report No. 215.
- 262 Kristensen, K., Nielsen, A., Berg, C. W., Skaug, H., and Bell, B. M. 2016. TMB: Automatic differentiation
263 and Laplace approximation. Journal of Statistical Software **70**(5): 1–21.
- 264 Miller, T. J. 2013. A comparison of hierarchical models for relative catch efficiency based on paired-gear
265 data for U.S. Northwest Atlantic fish stocks. Canadian Journal of Fisheries and Aquatic Sciences **70**(9):
266 1306–1316, doi: 10.1139/cjfas-2013-0136.
- 267 Miller, T. J., Martin, M., Politis, P., Legault, C. M., and Blaylock, J. 2017a. Some statistical approaches to
268 combine paired observations of chain sweep and rockhopper gear and catches from NEFSC and DFO trawl
269 surveys in estimating Georges Bank yellowtail flounder biomass. TRAC Working Paper 2017/XX. 36p.,
- 270 Miller, T. J., Politis, P., Blaylock, J., Richardson, D., Manderson, J., and Roebuck, C. 2018. Relative efficiency
271 of a chain sweep and the rockhopper sweep used for the NEFSC bottom trawl survey and chainsweep-based
272 swept area biomass estimates for 11 flatfish stocks. SAW 66 summer flounder Data/Model/Biological
273 Reference Point meeting. National Marine Fisheries Service, Northeast Fisheries Science Center, Woods
274 Hole, MA. September 17-21, 2018.
- 275 Miller, T. J., Richardson, D., Politis, P., Blaylock, J., Manderson, J., and Roebuck, C. 2020. SAW 66 summer
276 flounder Data/Model/Biological Reference Point meeting. National Marine Fisheries Service, Northeast
277 Fisheries Science Center, Woods Hole, MA. September 17-21, 2018.
- 278 Miller, T. J., Richardson, D. E., Politis, P., and Blaylock, J. 2017b. NEFSC bottom trawl catch efficiency and
279 biomass estimates for 2009-2017 for 8 flatfish stocks included in the 2017 Northeast Groundfish Operational
280 Assessments. 2017 Groundfish Operational Assessment working paper. Northeast Fisheries Science Center.
- 281 NEFSC. 2020. Operational assessment of 14 northeast groundfish stocks, updated through 2018. Prepublication
282 Copy of the September 2019 Operational Stock Assessment Report. The report is “in preparation” for

- 283 publication by the NEFSC. (Oct. 3, 2019; latest revision: Jan. 7, 2020). <https://nefsc.noaa.gov/saw/2019-groundfish-docs/Prepublication-NE-Grndfsh-1-7-2020.pdf>.
- 284
- 285 Politis, P. J., Galbraith, J. K., Kostovich, P., and Brown, R. W. 2014. Northeast Fisheries Science Center
286 bottom trawl survey protocols for the NOAA Ship Henry B. Bigelow. U.S. Dept. Commer., Northeast Fish.
287 Sci. Cent. Ref. Doc. 14-06, 138p.
- 288 R Core Team. 2019. R: A Language and Environment for Statistical Computing. R Foundation for Statistical
289 Computing, Vienna, Austria.
- 290 Smith, S. J. 1997. Bootstrap confidence limits for groundfish trawl survey estimates of mean abundance.
291 Canadian Journal of Fisheries and Aquatic Sciences 54(3): 616–630, doi: 10.1139/f96-303.
- 292 Wood, S. N. 2006. Generalized Additive Models: An Introduction with R. Chapman & Hall, Boca Raton,
293 Florida, 392 pp.

Fig. 1. Diagram of the standard Northeast Fisheries Science Center rockhopper sweep center and wing sections.

ROCKHOPPER CENTER SECTION
Section = 890cm, 100lbs Lead

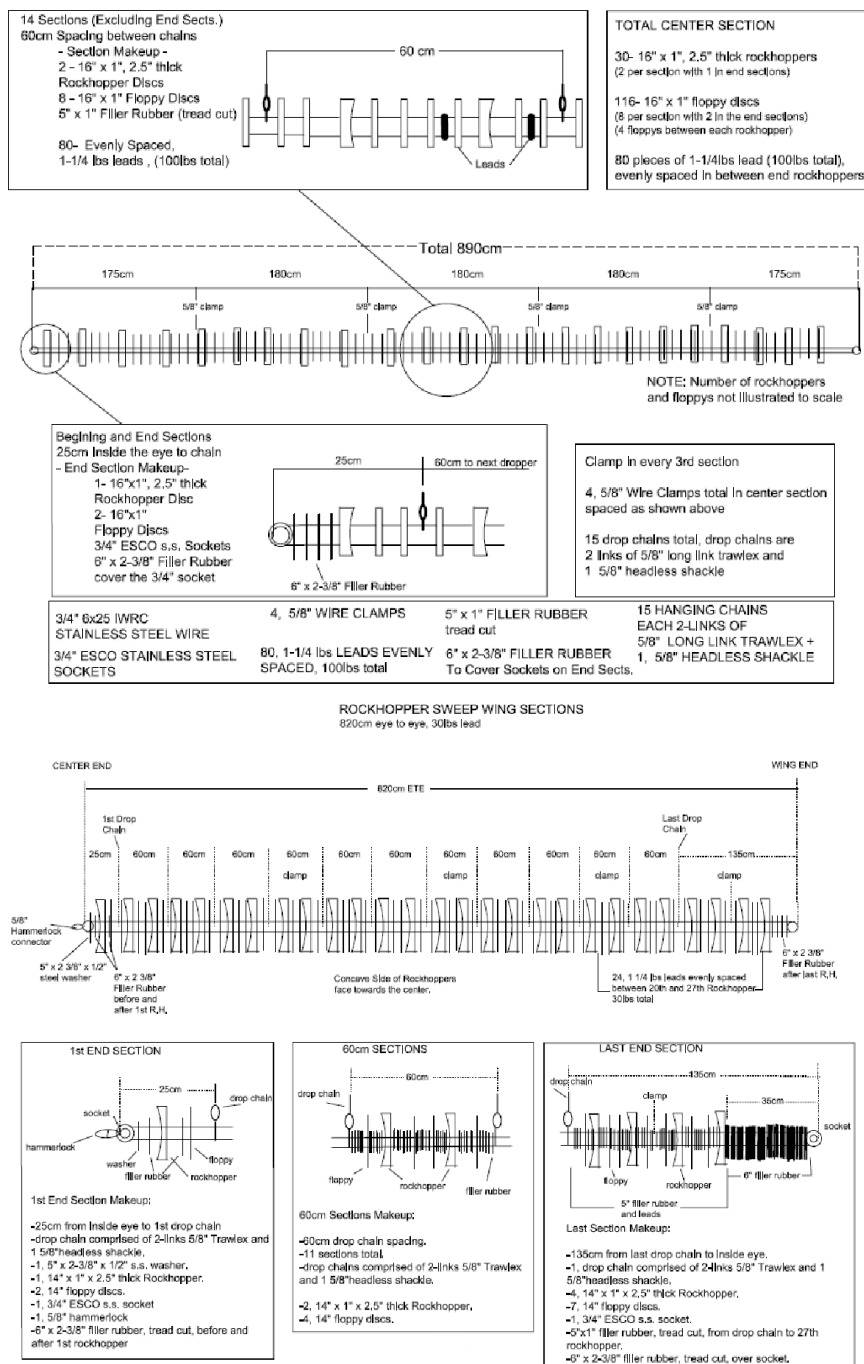


Fig. 2. Diagram of the chain sweep designed maximize bottom contact and flatfish capture.

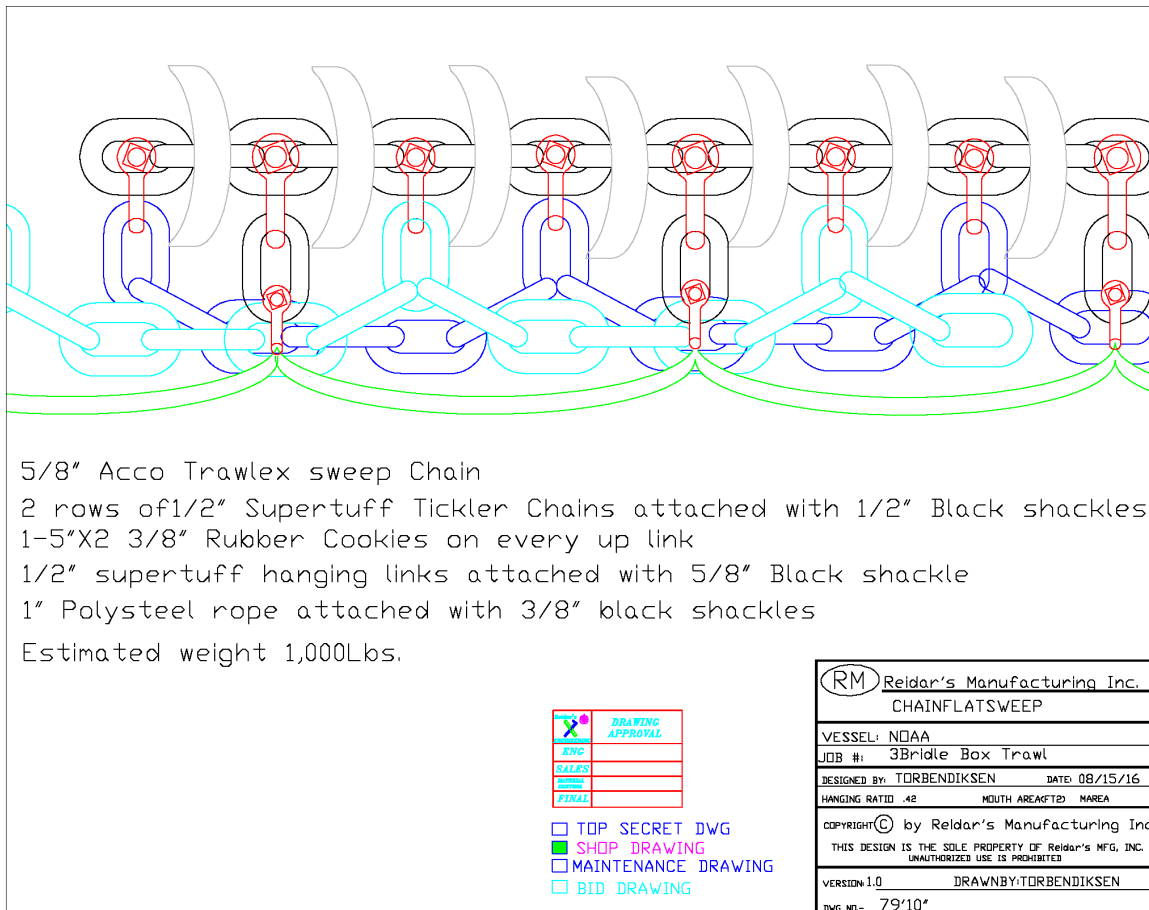


Fig. 3. Locations of stations in 2015 where the F/V Karen Elizabeth conducted twin-trawl sets with the standard bottom trawl gear and the gear with a chain sweep instead of the rockhopper sweep.

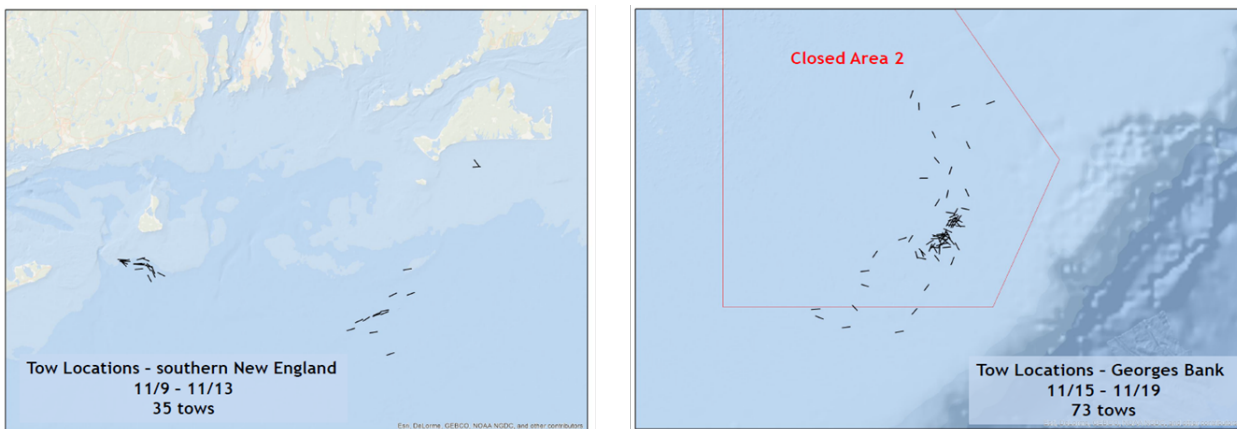


Fig. 4. Locations of stations in 2016 where the F/V Karen Elizabeth conducted twin-trawl sets with the standard bottom trawl gear and the gear with a chain sweep instead of the rockhopper sweep.

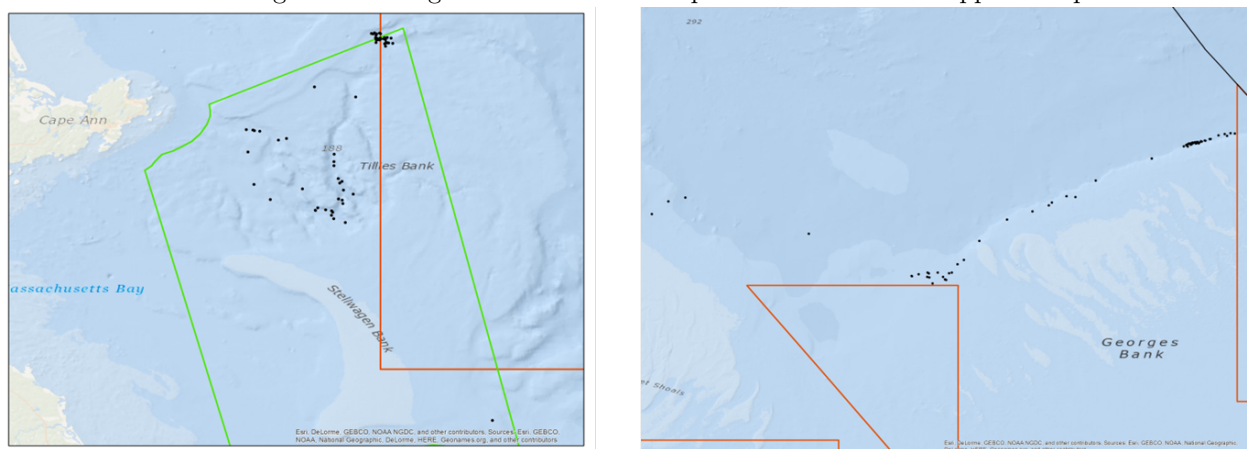


Fig. 5. Locations of stations in 2017 where the F/V Karen Elizabeth conducted twin-trawl sets with the standard bottom trawl gear and the gear with a chain sweep instead of the rockhopper sweep.

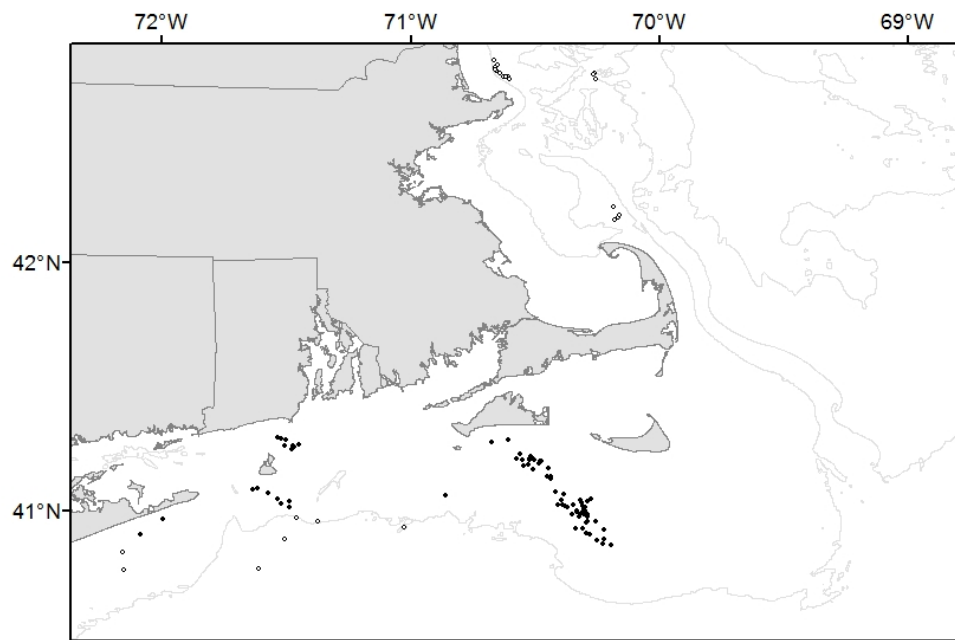


Fig. 6. Relative efficiency of gears using chain and rockhopper sweeps from the best performing model for each species (Table 4). Blue and red denote results for day and night data, respectively, and points represent empirical estimates of relative efficiency for each paired observation by length and paired tow. Polygons and dashed lines represent asymptotic and bootstrap-based 95% confidence intervals, respectively.

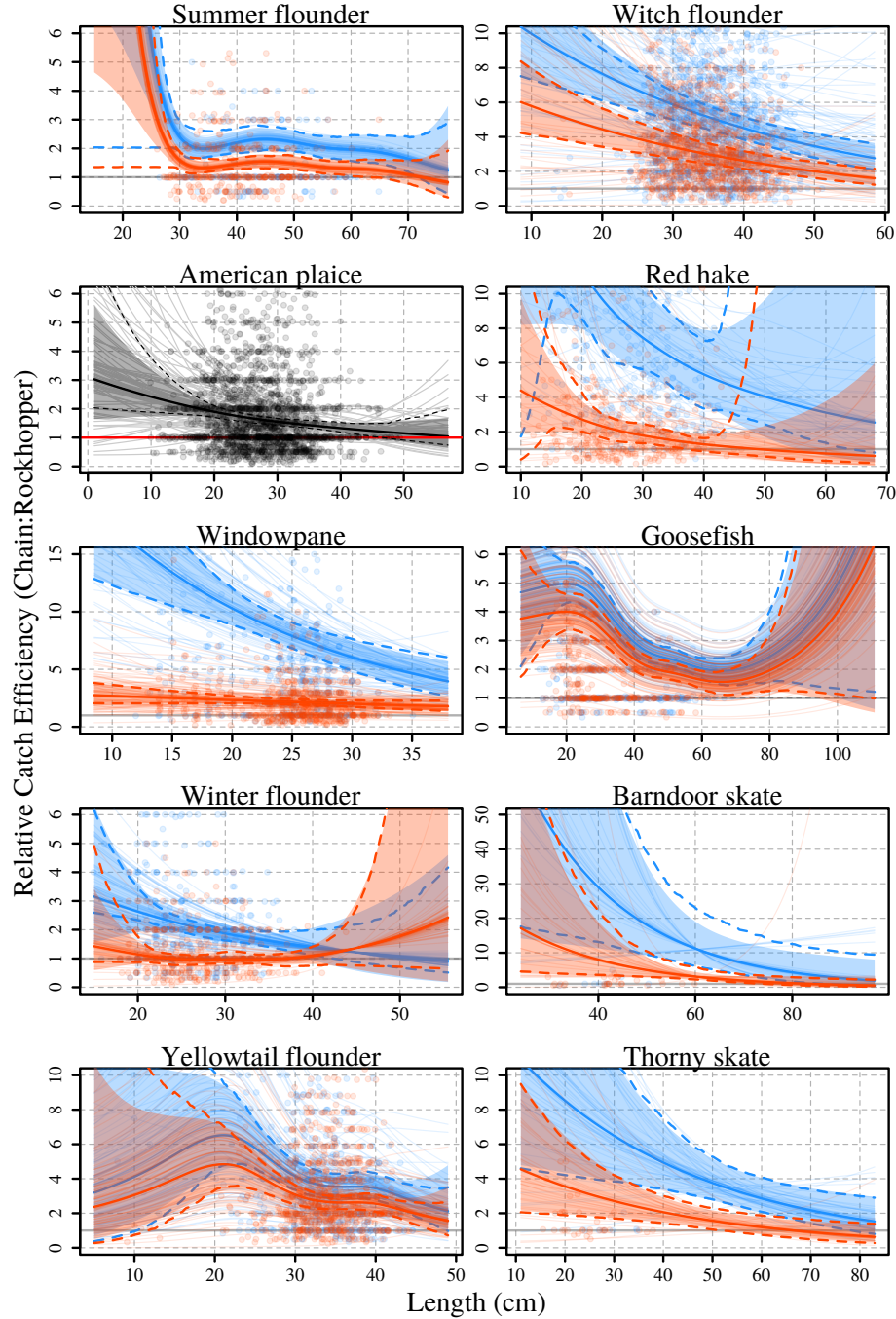


Table 1. Description of relative catch efficiency (ρ) and beta-binomial dispersion (ϕ) parameterizations for binomial and beta-binomial models and number of marginal likelihood parameters (n_p) for the 13 base models from Miller (2013) and fit to paired chainsweep and rockhoppersweep tow data for each species.

| Model | $\log(\rho)$ | $\log(\phi)$ | n_p | Description |
|-----------------|-----------------------------------|------------------|-------|--|
| BI ₀ | ~ 1 | – | 1 | population-level mean for all observations |
| BI ₁ | $\sim 1 + 1 pair$ | – | 2 | population- and random station-level ρ |
| BI ₂ | $\sim s(length)$ | – | 3 | population-level smooth size effect on ρ |
| BI ₃ | $\sim s(length) + 1 pair$ | – | 4 | population-level smooth size effect and random station-level intercept for ρ |
| BI ₄ | $\sim s(length) + s(length) pair$ | – | 7 | population-level and random station-level smooth size effects for ρ |
| BB ₀ | ~ 1 | ~ 1 | 2 | population-level ρ and ϕ |
| BB ₁ | $\sim 1 + 1 pair$ | ~ 1 | 3 | population-level and random station-level intercept for ρ and population-level ϕ |
| BB ₂ | $\sim s(length)$ | ~ 1 | 4 | population-level smooth size effect on ρ and population-level ϕ |
| BB ₃ | $\sim s(length)$ | $\sim s(length)$ | 6 | population-level smooth size effect on ρ and ϕ |
| BB ₄ | $\sim s(length) + 1 pair$ | ~ 1 | 5 | population-level smooth size effect and random station-level intercept for ρ and population-level ϕ |
| BB ₅ | $\sim s(length) + 1 pair$ | $\sim s(length)$ | 7 | population-level smooth size effect on ρ and ϕ and random station-level intercepts for ρ |
| BB ₆ | $\sim s(length) + s(length) pair$ | ~ 1 | 8 | population-level and random station-level smooth size effects on ρ and population-level ϕ |
| BB ₇ | $\sim s(length) + s(length) pair$ | $\sim s(length)$ | 10 | population-level and random station-level smooth size effects on ρ and population-level smooth size effects on ϕ |

Table 2. Number of paired tows where fish were captured and the number of fish captured and measured for lengths for each species in total and by day or night.

| Species | Paired Tows | | | Captured | Both Gears Measured | | | Chainsweep Measured | | | Rockhopper Measured | | |
|---------------------|-------------|-----|-------|----------|---------------------|--------|--------|---------------------|-------|-------|---------------------|-------|-------|
| | Total | Day | Night | | Total | Day | Night | Total | Day | Night | Total | Day | Night |
| Summer flounder | 141 | 75 | 66 | 4,154 | 4,154 | 1,770 | 2,384 | 2,616 | 1,195 | 1,421 | 1,538 | 575 | 963 |
| American plaice | 134 | 84 | 50 | 31,983 | 19,245 | 13,619 | 5,626 | 10,982 | 7,775 | 3,207 | 8,263 | 5,844 | 2,419 |
| Windowpane | 195 | 100 | 95 | 15,310 | 13,014 | 6,221 | 6,793 | 9,854 | 5,443 | 4,411 | 3,160 | 778 | 2,382 |
| Winter flounder | 171 | 97 | 74 | 6,586 | 6,449 | 3,605 | 2,844 | 3,805 | 2,385 | 1,420 | 2,644 | 1,220 | 1,424 |
| Yellowtail flounder | 192 | 101 | 91 | 18,545 | 14,134 | 6,849 | 7,285 | 10,065 | 5,297 | 4,768 | 4,069 | 1,552 | 2,517 |
| Witch flounder | 132 | 83 | 49 | 57,133 | 23,927 | 13,899 | 10,028 | 14,899 | 9,271 | 5,628 | 9,028 | 4,628 | 4,400 |
| Red hake | 73 | 40 | 33 | 47,275 | 12,585 | 6,614 | 5,971 | 8,587 | 4,908 | 3,679 | 3,998 | 1,706 | 2,292 |
| Goosefish | 302 | 165 | 137 | 8,798 | 8,541 | 3,985 | 4,556 | 6,409 | 3,053 | 3,356 | 2,132 | 932 | 1,200 |
| Barndoor skate | 62 | 33 | 29 | 502 | 502 | 219 | 283 | 397 | 198 | 199 | 105 | 21 | 84 |
| Thorny skate | 90 | 56 | 34 | 907 | 907 | 399 | 508 | 648 | 311 | 337 | 259 | 88 | 171 |

Table 3. Difference in AIC for each of the 13 models described in Table 1 from the best model (**0**) by species.

| | BI ₀ | BI ₁ | BI ₂ | BI ₃ | BI ₄ | BB ₀ | BB ₁ | BB ₂ | BB ₃ | BB ₄ | BB ₅ | BB ₆ | BB ₇ |
|---------------------|-----------------|-----------------|-----------------|-----------------|-----------------|-----------------|-----------------|-----------------|-----------------|-----------------|-----------------|-----------------|-----------------|
| Summer flounder | 27.96 | 13.53 | 8.9 | 0 | | 28.64 | 15.45 | 10.59 | | | | | |
| American plaice | 821.11 | 546.54 | 743.34 | 494.92 | 415.63 | 179.48 | 71.76 | 141.44 | | 37.06 | 0.71 | 0 | |
| Windowpane | 1045.06 | 38.51 | 1029.72 | 17.03 | 0 | 585.7 | 32.22 | 572.73 | | 15.27 | | | |
| Winter flounder | 216.47 | 15.73 | 200.33 | 3.02 | 0 | 163.31 | 16.63 | 151.66 | 151.01 | 4.21 | 6.78 | 1.41 | |
| Yellowtail flounder | 727.15 | 97.93 | 727.36 | 51.84 | 10.96 | 394.94 | 70.2 | 391.13 | 371.13 | 31.85 | 0 | 3.33 | |
| Witch flounder | 1424.17 | 212.64 | 1372.66 | | 35.33 | 881.28 | 142.53 | 844.47 | | 81.37 | 0 | | |
| Red hake | 1884.51 | 295.85 | | 170.75 | | 627.33 | 166.43 | 590.92 | | 95.8 | 59.31 | 0 | 0.83 |
| Goosefish | 227.67 | 87.23 | 80.37 | 0 | | 219.13 | | 76.54 | | | | | |
| Barndoor skate | 36.51 | 10.01 | 31.34 | 2.72 | 0 | 36.23 | 11.99 | 29.03 | | 4.6 | | | |
| Thorny skate | 39.04 | 8.57 | 32.65 | 3.44 | 1.15 | 22.38 | 5.84 | 18.66 | | 1.38 | 5.19 | 0 | |

Table 4. Best performing models from Table 3 and extended models that include diel effects on relative catch efficiency for each species with the number of parameters for each model (n_p) and the differences in AIC (ΔAIC) from the best of the three models (**0**) by species.

| | Model | $\log(\rho)$ | $\log(\phi)$ | n_p | ΔAIC |
|----------------------------|------------------|---|-------------------------|-------|--------------------|
| Summer flounder | | | | | |
| | BI ₃ | $\sim s(\text{length}) + 1 \text{pair}$ | – | 4 | 22.92 |
| | BI _{3a} | $\sim dn + s(\text{length}) + 1 \text{pair}$ | – | 5 | 0 |
| | BI _{3b} | $\sim dn * s(\text{length}) + 1 \text{pair}$ | – | 7 | 1.74 |
| American plaice | | | | | |
| | BB ₇ | $\sim s(\text{length}) + s(\text{length}) \text{pair}$ | $\sim s(\text{length})$ | 10 | 0 |
| | BB _{7a} | $\sim dn + s(\text{length}) + s(\text{length}) \text{pair}$ | $\sim s(\text{length})$ | 11 | 1.43 |
| | BB _{7b} | $\sim dn * s(\text{length}) + s(\text{length}) \text{pair}$ | $\sim s(\text{length})$ | 13 | 2.95 |
| Windowpane | | | | | |
| | BI ₄ | $\sim s(\text{length}) + s(\text{length}) \text{pair}$ | – | 7 | 152.1 |
| | BI _{4a} | $\sim dn + \text{length} + s(\text{length}) \text{pair}$ | – | 7 | 4.06 |
| | BI _{4b} | $\sim dn * \text{length} + s(\text{length}) \text{pair}$ | – | 8 | 0 |
| Winter flounder | | | | | |
| | BI ₄ | $\sim s(\text{length}) + s(\text{length}) \text{pair}$ | – | 7 | 50.68 |
| | BI _{4a} | $\sim dn + s(\text{length}) + \text{length} \text{pair}$ | – | 7 | 0.3 |
| | BI _{4b} | $\sim dn * s(\text{length}) + \text{length} \text{pair}$ | – | 9 | 0 |
| Yellowtail flounder | | | | | |
| | BB ₆ | $\sim s(\text{length}) + s(\text{length}) \text{pair}$ | ~ 1 | 8 | 3.84 |
| | BB _{6a} | $\sim dn + s(\text{length}) + s(\text{length}) \text{pair}$ | ~ 1 | 9 | 0 |
| | BB _{6b} | $\sim dn * s(\text{length}) + s(\text{length}) \text{pair}$ | ~ 1 | 11 | 3.48 |
| Witch flounder | | | | | |
| | BB ₆ | $\sim s(\text{length}) + s(\text{length}) \text{pair}$ | ~ 1 | 8 | 19.68 |
| | BB _{6a} | $\sim dn + \text{length} + s(\text{length}) \text{pair}$ | ~ 1 | 8 | 0 |
| | BB _{6b} | $\sim dn * \text{length} + s(\text{length}) \text{pair}$ | ~ 1 | 9 | 1.52 |
| Red hake | | | | | |
| | BB ₆ | $\sim s(\text{length}) + s(\text{length}) \text{pair}$ | ~ 1 | 8 | 32.35 |
| | BB _{6a} | $\sim dn + s(\text{length}) + s(\text{length}) \text{pair}$ | ~ 1 | 8 | 0 |
| | BB _{6b} | $\sim dn * s(\text{length}) + s(\text{length}) \text{pair}$ | ~ 1 | 10 | 3.18 |
| Goosefish | | | | | |
| | BI ₃ | $\sim s(\text{length}) + 1 \text{pair}$ | – | 4 | 5.44 |
| | BI _{3a} | $\sim dn + s(\text{length}) + 1 \text{pair}$ | – | 5 | 0 |
| | BI _{3b} | $\sim dn * s(\text{length}) + 1 \text{pair}$ | – | 7 | 6.8 |
| Barndoor skate | | | | | |
| | BI ₄ | $\sim s(\text{length}) + s(\text{length}) \text{pair}$ | – | 7 | 15.57 |
| | BI _{4a} | $\sim dn + \text{length} + \text{length} \text{pair}$ | – | 5 | 0 |
| | BI _{4b} | $\sim dn * \text{length} + \text{length} \text{pair}$ | – | 6 | 1.83 |
| Thorny skate | | | | | |
| | BB ₆ | $\sim s(\text{length}) + s(\text{length}) \text{pair}$ | ~ 1 | 8 | 15.51 |
| | BB _{6a} | $\sim dn + \text{length} + \text{length} \text{pair}$ | ~ 1 | 7 | 0 |
| | BB _{6b} | $\sim dn * \text{length} + \text{length} \text{pair}$ | ~ 1 | 8 | 1.38 |